iJRASET
International Journal For Research in Applied Science and Engineering Technology

INTERNATIONAL JOURNAL FOR RESEARCH

IN APPLIED SCIENCE & ENGINEERING TECHNOLOGY

Volume: 12 **Issue:** VI **Month of publication:** June 2024

DOI: https://doi.org/10.22214/ijraset.2024.63184

www.ijraset.com

Call: 08813907089 | E-mail ID: ijraset@gmail.com

International Journal for Research in Applied Science & Engineering Technology (IJRASET)
ISSN: 2321-9653; IC Value: 45.98; SJ Impact Factor: 7.538
Volume 12 Issue VI June 2024- Available at www.ijraset.com

Friction Stir Welding Benefits Technique over Other Welding Techniques of Dissimilar Metals

Vikas C M[1], Bheemkumar Haloor[3], Lakshmi Kiran C M[2], Arvind Ashok Ghulanur[3], Vaishnavi Raga[3], Supriya B K[4], Apoorva D K[3], Sushma K[5]

[1]*Department of Mechanical Engineering, PES College of Engineering, Mandya, Karnataka, India*
[2]*Department of Computer Science Engineering, PES College of Engineering, Mandya, Karnataka, India*
[3]*Department of Electrical and Electronics Engineering, PES College of Engineering, Mandya, Karnataka, India*
[4]*Department of Information Science Engineering, PES College of Engineering, Mandya, Karnataka, India*
[5]*Department of Information Science Engineering, B.E.T Polytechnic, Bhartinagar, Karnataka, India*

Abstract: ***Due to the low heat input situation, solid state welding (SSW) has demonstrated higher potential for integrating a variety of equivalent and dissimilar material combinations. The temperature stays below the melting point of the source materials throughout the solid-state welding process. Compared to fusion welding, solid state welding offers the highest quality. Aeronautics, nuclear, space, and aviation are just a few of the industrial production sectors that utilize the solid-state welding technology. Diffusion welding, explosion welding, friction welding, forge welding, cold welding, role welding, hot pressure welding, and ultrasonic welding are just a few of the SSW techniques covered in the current article. This study looks at a variety of SSW kinds and solid-state welding applications. This study examines many types of SSW and the applications of solid-state welding. Current Study includes the pros and cons of other welding techniques over friction stir welding.***

I. INTRODUCTION

The Welding Institute (TWI) in Cambridge, United Kingdom, invented the FRICTION stir welding (FSW) method in 1991. The FSW technique's energy efficiency, environmental friendliness, and adaptability have made it the most significant advancement in metal joining in recent years. High- strength aerospace aluminum alloys and other metal alloys that are challenging to fuse using traditional fusion welding processes can be joined using this method[1].

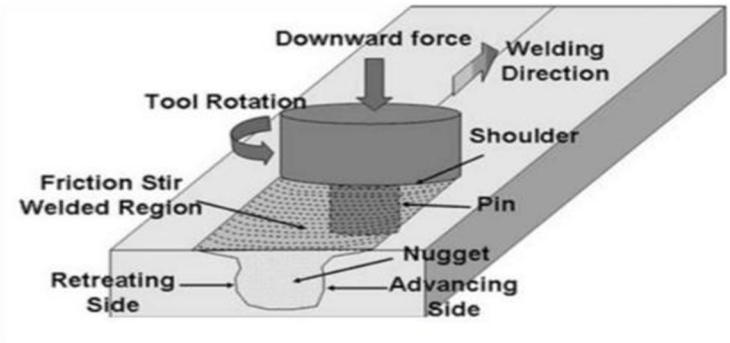

Fig.1- Schematic drawing of FSW

Initially, this joining technique was employed to unite aluminum alloys, such as alloys 2xxx or 7xxx, which were challenging to fuse using conventional fusion welding techniques. Later, it was used to a wide range of materials, such as polymers, titanium alloys, magnesium, copper, nickel, steel composites, and even nickel, copper, and nickel alloys.

Based on the thermo-mechanical histories they have through, the heat affected zone (HAZ), the thermo-mechanical impacted zone (TMAZ), and the stir zone (SZ) in a friction stirred joint may all be identified.

The heat-affected zones (HAZ, TMAZ, and SZ) are expected to experience precipitate formation or dissolution (for example, in aluminum alloys) as well as phase transitions (for instance, in steels or titanium alloys). The phase transition will no longer be discussed in this study because it occurs in the base materials as a result of heating and has no direct bearing on welding of dissimilar metals[2].

Both composite materials were successfully joined using FSW techniques. The microstructures of the Al-Al2O3 and Al-SiC composites from various regions[3].

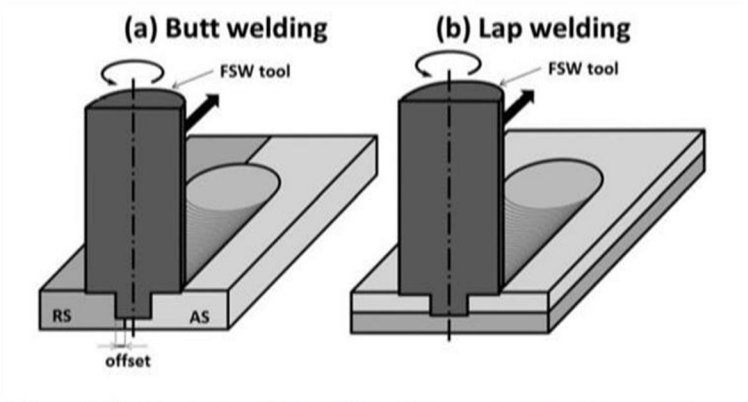

Fig.2- Dissimilar friction stir welding for (a)Butt and (b) lap welds. As, advancing side; RS, retreating side.

II. FRICTION-STIR FINE-GRAINED STRUCTURE

All that takes place during dynamic recrystallization in the stirred zone (SZ). In this instance, the SZ resulted in recrystallized grains that were fine, equiaxed, and generally homogeneous in size. Figure 2 depicts the typical microstructure of FSP 7075AlT651. At 400 rpm for the tool and 102 mm/min for the traverse, a fine-grained microstructure of around 7.5 lm was created. Even said, there is still disagreement on the SZ's technique for refining grains. The SZ's FSP settings, tool geometry, material chemistry, workpiece temperature, vertical pressure, and active cooling have a major impact on the size of the recrystallized grains[3].

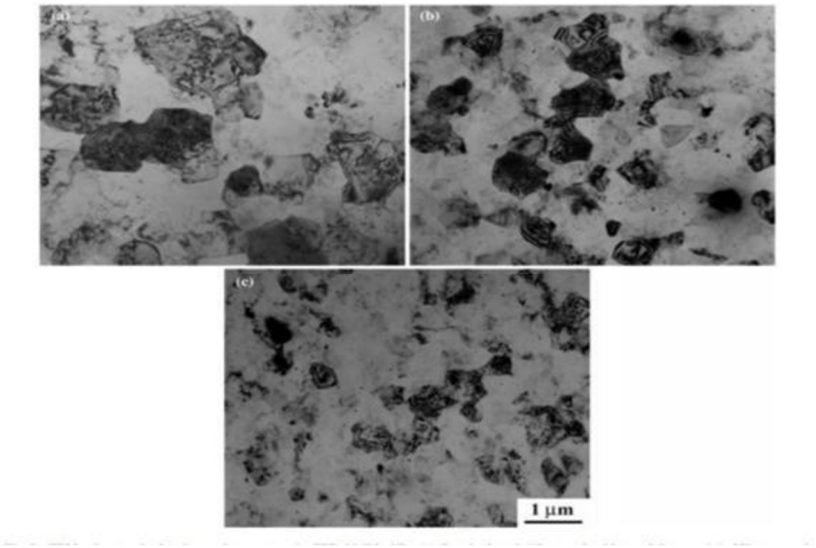

Fig. 3: A TEM image of FSP Al-4Mg-lZr

Illustrating the grain structure. Standard tool (18mm, shoulder, and 8mm pin), 350 rpm, 203 mm/min; enhanced tool (12mm, shoulder, and 4mm pin), 600 rpm, 25 mm/min; and upgraded tool (12mm, shoulder, and 4mm pin), 300 rpm, 203 mm/min.

III. FRICTION-STIR SURFACE/BULK COMPOSITE

The first result of a SiCp-Al surface composite in the FSW. Before applying the SiC powder to the plates, a little quantity of methanol was mixed in to provide an equal and thin coating. FSP was applied to aluminum plates that already had a coating of SiC particles on them. On substrates made of the 5083Al and A356 aluminum alloys, a composite layer of around 100 lm was produced using the best tool design and processing conditions.Fig.4 shows the surface composite. layers created by FSP in (a) A356 and (b) 5083 Al substrates with SiC particle volume fractions of 15 and 13, respectively.

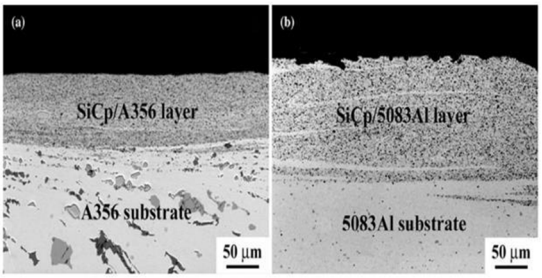

Fig.4- Visualization of surface composite.

By adjusting the FSP parameters, 5 to 27 vol pct of the SiC particles may be incorporated into the aluminum matrix. The HV of the surface layer of aluminum substrates was significantly enhanced by the addition of SiC particles, and it increased as the volume percent of SiC particles increased for the FSP SiCp/5083Al surface composite.

Adding 15 vol pct SiC through FSP to the surface layer of A356 increased the HV from 98 to 171. This is similar to adding 15 vol pct SiC through FSP to the surface layer of SiCp/5083Al surface composite layers created using FSP: Variation in hardness with SiC particle volume%[1].

IV. METHODOLOGY EXPERIMENTAL PROCEDURE

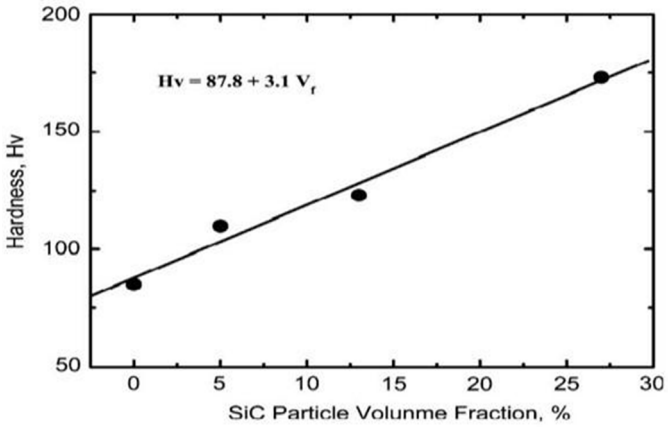

Fig. 5- Aluminum metal matrix composition

The casting procedure was used to create two different kinds of metal-matrix composites for this experiment. The first kind is created using a 6061-alloy matrix with 20 volume percent Al2O3 reinforcement particles. The alloy had reached the solutionization stage. Al0.6Si-0.28Cu-1.0Mg-0.2Cr (wt pct) is the nominal chemical make-up of 6061 alloy. ALCAN International, a company based in the United States, provided the composite. Slices of the samples, each 0.75 inches (19.76 mm) thick, were accessible. After that, the parts were divided into 4- mm-thick plates of thinness. Throughout this work, this sample will be referred to as the Al-Al2O3 composite.

In order to create the second type of composite, a 20 vol pct silicon carbide (SiC) whisker is dispersed throughout a 2124 alloy matrix. The buyer received the alloys in excellent shape. The nominal chemical make-up of the 2124 alloy is Al- 4.4Cu0.6Mn-1.5Mg (wt pct). The large plate was divided into pieces that were each 4 mm thick. In this text, this sample will be referred to as the Al- SiC composite.

With the use of this technique, the matrix could be thoroughly dispersed, providing a clear view of the SiC whisker orientation. The OIM was primarily used to assess the orientation of the SiC whisker in the base metal (BM) and the friction stir welded region. The microstructures of the heat-affected zone and the friction stir-welded area of the Al-SiC composites were examined using the TEM (HAZ). Ion-beam thinning was used to create the TEM samples. PHILIPS* CM-12 transmission electron microscope was used for the TEM.

ISSN: 2321-9653; IC Value: 45.98; SJ Impact Factor: 7.538
Volume 12 Issue VI June 2024- Available at www.ijraset.com

V. RESULT

The two composite materials were effectively connected using FSW techniques. Here, the microstructures of the composites made of Al- Al2O3 and Al-SiC are shown. Al2O3 particles with an angular shape and a 20 m diameter can be seen in the BM microstructures of the Al-Al2O3 composites (Figure 6(a)). The macrostructure displayed three unique regions: the directionally recrystallized area (DXZ) near the centre of the joint, the TMAZ, and the HAZ. There were little differences between the microstructures from the BM and the HAZ. The presence of smaller particles in the microstructure from the TMAZ provided an indication of Al2O3 particle breakage (Figure 6(b)). In addition, it appears that these tiny particles are broken up, which results in the formation of bands.

There were no discernible variations in the course particulate distributions between the BM and the DXZ zone, save from the presence of tiny particles (Figure 6(c)). The measured hardness values for the DXZ, TMAZ, HAZ, and BM areas are shown in Figure 7. The BM and DXZ zones' hardness readings (between 100 and 140 HV) were equivalent. Figure 7 shows how the Al2O3 particle clustering caused a considerable increase in hardness (200 HV) in the TMAZ areas.

Figure 6 compares the microstructures of the Al-SiC composites from various areas. The BM microstructure contains whiskers in various orientations, as seen in Figure 6(a). Early processing of these composites was the subject of cursory research, which revealed that the predominant orientation of the SiC whiskers in the base material was in the x direction. The microstructure from the DXZ region is similar to that from the BM region in Figure 6(c), with a little propensity for the whiskers to cluster together as seen by the series of arrows. In the TMAZ/DXZ boundary areas, the principal axes of the SiC whiskers seem to be aligned with the welding direction (Figure 6(b)). This phenomenon is examined in further depth using SEM.

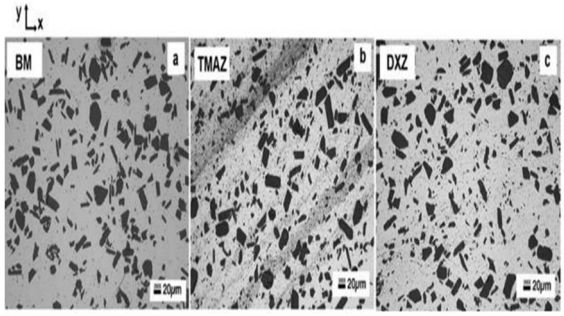

Fig. 6- BM microstructures of the Al-Al2O3 composites

Figure 6 compares optical micrographs of a friction stir weld created on Al-Al2O3 composites: the BM area, the TMAZ zone, which demonstrates the bimodal nature of particles and the segregation of tiny particles along bands, and the AXZ region, which demonstrates the coexistence of coarse and fine particles. The plane of the micrographs is in the direction x and y, while the welding direction is in the z direction, which is perpendicular to x and y.

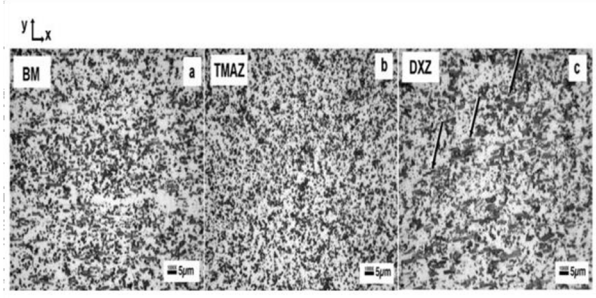

Fig. 7- Microstructures of the Al-SiC composites

Fig. 8: Comparison of optical micrographs taken during friction stir welds on Al-SiC composites in the BM area, TMAZ region, and DXZ zone. What appears to be a change in the SiC orientation is seen in Fig. 7(b). The cluster of SiC whiskers that appears in Fig. 7(c) is indicated by the row of arrows. In the direction of z, which is in the plane of the micrographs, the welding route is perpendicular to the x-y plane.

The DXZ areas are somewhat softer than the BM (Figure 3(b)) regions, according to the measured hardness over the joint region (Figure 10(a)) (170 to 190 HV). In comparison to the TMAZ and HAZ zones, the DXZ region (133 to 160 HV) was a little softer. The automated indenter testing instrument (b) also identifies spatial changes in hardness, which are shown in Figure 10. The findings demonstrate that the distribution of hardness variations over the DXZ is not constant. These geographical heterogeneities are thought to be the outcome of various metal fluxes occurring in various places.

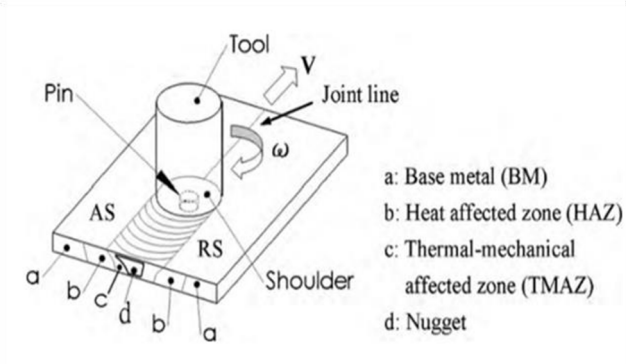

Fig.8- Schematic diagram of an FSW process

Fig. 8-(a) shows measured hardness values on Al-SiC composites plotted against distance from the friction stir weld's center. The spatial hardness distribution shows that there is microstructural diversity even within the DXZ when measured across a larger area that encompasses the TMAZ and DXZ sections[4].

VI. EXPERIMENTAL STUDY ON FRICTION STIR WELDING OF COPPER METALS

The DXZ areas are somewhat softer than the BM (Figure 3(b)) regions, according to the measured hardness over the joint region (Figure 10(a)) (170 to 190 HV). In comparison to the TMAZ and HAZ zones, the DXZ region (133 to 160 HV) was a little softer. The automated indenter testing instrument (b) also identifies spatial changes in hardness, which are shown in Figure 10. The findings demonstrate that the distribution of hardness variations over the DXZ is not constant. It is hypothesized that the different metal fluxes occurring in different places are what caused these spatial heterogeneities.

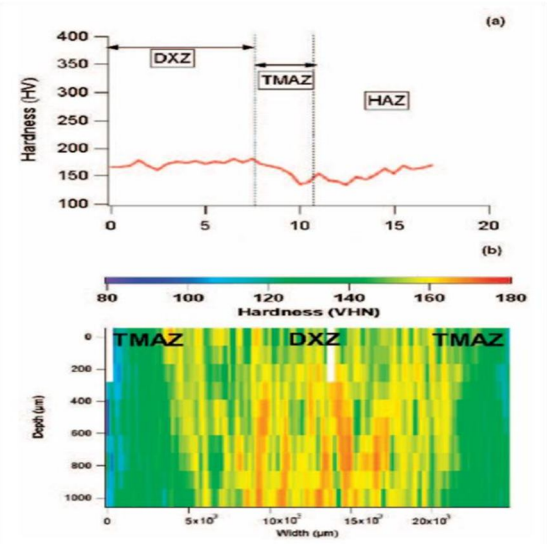

Fig. 9: Comparison of optical micrographs taken during friction stir welds on Al-SiC composites.

Once the weld is complete and the pin of the welding tool is removed, a hole is left in the workpiece. Frictional heat is created when the shoulder is pressed on the surface of the workpiece. Thus, the pin contributes to the production of heat and greatly boosts the workpiece's plastic flow. The four zones that may be utilized to classify the microstructure along the joint line are BM, HAZ, TMAZ, and Nugget, as shown in Fig. 1.

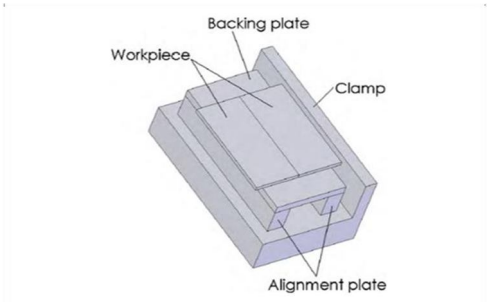

Fig.10- Configuration of the workpiece and fixture table.

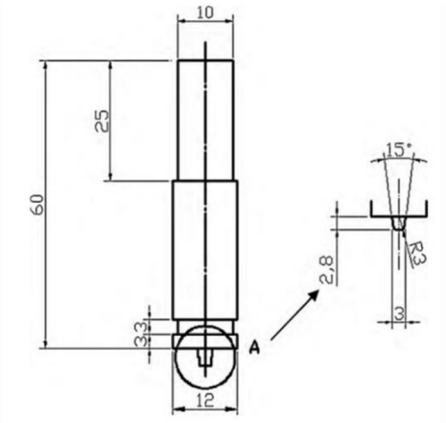

Fig.11- Dimensions of the tool and pin

For the welding trials, two different types of welding circumstances (a) = 800 rpm, v = 30 mm/min and (b) = 900 rpm, v = 50 mm/min were used. The pin is initially inserted into the workpiece during the FSW process to a depth of 2.85 mm. The downward force is at around 4 kN. The expansion of the heated metal causes the downward force to rise to around 7 kN after the temperature reaches about 400 C. The downward force must be kept under 10 kN due to the FSW machine's capacity restriction. Fig. 5 depicts how a welded product with condition (b) looks.

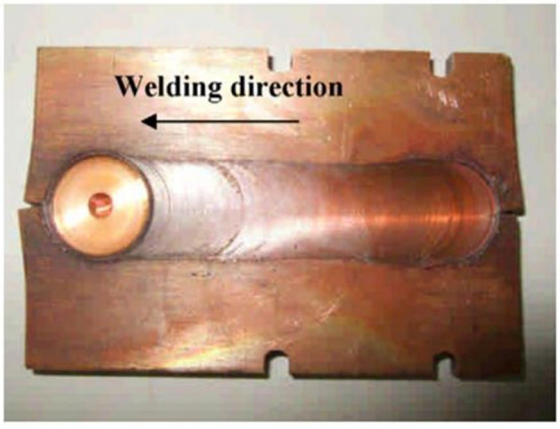

Fig.12- Appearance of a welded product for ω=900 rpm and v=50 mm/min.

Photos of the test parts taken after tensile testing under welding circumstances are shown in Fig. 10. The figure demonstrates that the necking zone for the base metal and the weld at condition typically occurred at the midpoint of the test piece. On the other hand, the necking zone for the test piece was at the HAZ at condition.

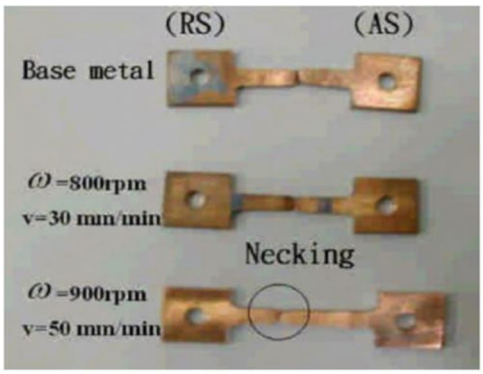

Fig.13- Appearance of the test piece after tensile tests.

Figs. 14(a), (b), and (c) show the microstructures of the BM, HAZ, and Nugget, respectively. The crystal size (about 10 m) is seen from Fig. 14(a). The HAZ shown in Fig. 14(b) saw an increase in mean crystal size as a result of annealing effects. Smaller crystals developed in Fig. 14(c) due to dynamic recovery and stirring effects, which resulted in greater elongation than the BM, as observed in Fig.11.Scale bars are seen in the figures. Nuggets on AS and RS have microstructures that are around the same size.[5]

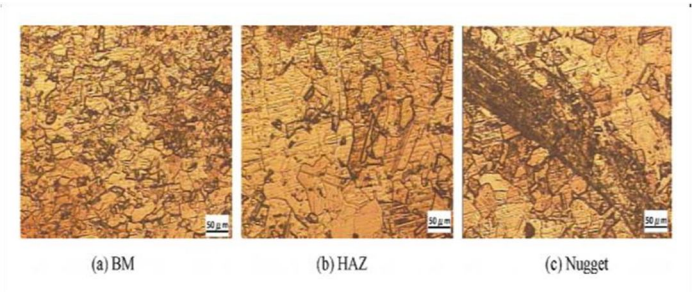

Fig.15- Microstructure of the welds in different zones.

VII. DIFFERENT WELDING TECHNIQUES

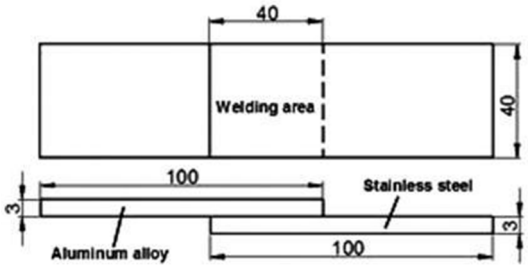

Fig.16- configuration and dimensions of the joints[3].

Diffusion welding is a technology where the materials are fused to join by heating them to their melting temperature. Two clean and flat surfaces are brought into contact and then joined. Diffusion welding enlarges the bonding procedures domain because of the multiple combinations. 2- types of Diffusion welding process-solid state and liquid state. Solid state welding process-the material is joined by a plastic deformation process where Diffusion starts in the solid phase. The bonding takes place when a welding temperature is lower than the melting temperature of both materials. The welding temperature must be 50%-80% of the melting temperature of the metals. Liquid phase Diffusion welding-this technique is applicable only to dissimilar materials or where dissimilar metals insert is used. The bonding temperature is selected as the temperature at which this phase melts. This technique is used particularly for metals like aluminum alloys where EUTECTICS points are formed[11].

ISSN: 2321-9653; IC Value: 45.98; SJ Impact Factor: 7.538
Volume 12 Issue VI June 2024- Available at www.ijraset.com

VIII. EXPERIMENTAL MATERIALS AND PROCESS

A. Martensitic Stainless Steels +Ductile Cast Iron

Martensitic stainless steels mainly consist of 10.5% of cr and other austenite stability elements, like carbon nitrogen nickel and manganese. Here in stainless steel the stabilizing elements used to expand the austerity phase and the composition of these elements should be in a balanced way to prevent DELTA-FERRITE formation at the automatizing temperature. DUCTILE CAST IRON - mainly consists of 3.4% c, some amount of Si and mn. Here manganese is sometimes avoided because it can reduce the impact resistance during welding. When we weld or fuse these materials or specimens and tested and then did some analysis in the cast iron side it is formed or printed with 2% natal and in stainless steel is printed with vilella's reagent[12]. After the oxides on their surfaces had been removed using abrasive paper, the surfaces of aluminum alloy sheet and stainless-steel sheet were washed with acetone to remove oil and residue prior to welding. Following welding, the joint was removed from the welded zone perpendicular to the welding contact, and the resultant specimen was ground and polished. Before cutting, the joint was covered with resin to safeguard it from damage during the machining process[13].

B. Ultrasonic Welding And Effects

Heat is produced during ultrasonic welding when plastic is repeatedly stretched. The loss modulus and cyclic strain amplitude of the polymer will affect the power dissipated. As a result, high strain amplitude areas heat up more quickly.
Because of two factors, static pressure is used in ultrasonic welding or applied to the workpieces in this process:

- To improve energy transfer by ensuring good contact between the horn and the components.
- To trigger the energy to flow, leading to the fusing of the component parts[15].

C. Effect Of Weld Time On Strength

ABS and PS -STRENGTH increases when the weld time is 2.4s. if it is greater than 2.4s strength will decreases. BECAUSE The length of the samples is close to quarter wavelength and the vibration amplitude at the joint is small[15]. For ABS and PS increasing in welding time up to 0.8s strength also increases but after 0.8s the effect cannot be tested for these metals. BECAUSE the geometry of the sample and the fixture. And it is expected that strength will be constant with increasing weld time[17]. Welding efficiency increases with weld time because due to the more ultrasonic energy dissipation at the interphase of the welding[16].

D. Effect of Collapse

Increased weld time also results in more collapse. Due to the flow of polymer meta[15]. As additional polymer melts and flows, lengthening the weld duration also lengthens the collapse. Because it also considers the fixtures, unfavorable molecular orientation, and compressibility of the pieces, the collapse is bigger than the height of the energy director as depicted. During welding, a correlation between collapse and strength and energy and strength was seen, showing that these characteristics may tell you a lot about the connection. According to the fig. above, widespread flow occurs for longer weld times because the collapse sharply rises with weld time. This user interfaces.

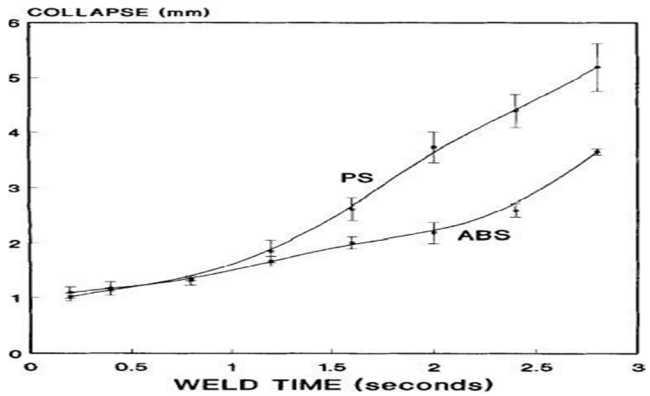

Fig.17- Effect of weld time on collaps

E. Effect Of Pressure

Due to the parallel alignment of the molecular chains, welding pressure increases but welding efficiency falls[16]. Increases in pressure lead to more collapse because low pressure might lead to poor horn to part contact and inefficient energy transfer. cause the molten energy director to flow inefficiently as well[17]. Parent material strength divided by welding strength equals welding efficiency[16]. As weld pressure increases, welding efficiency drops. The chain molecular parallel alignment stated earlier grows as weld pressure rises. Because the hold pressure has a very small impact on the effectiveness of welding[16].

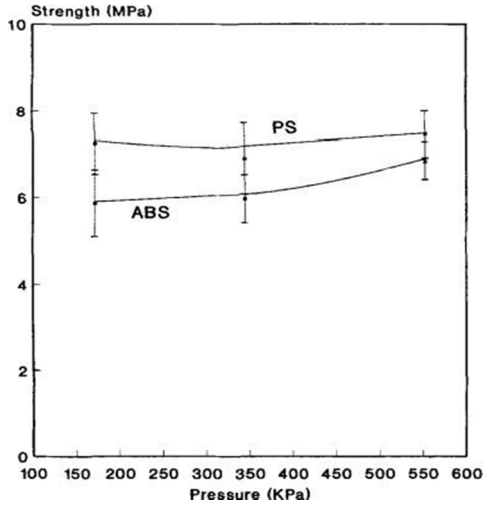

Fig.18- Effect of pressure on weld strength

F. Explosion Welding

Along with explosive welding, waves form on the weld border. Explosion welding entails identifying the elements that ensure wave creation at the weld boundary. The physical mechanisms that result in wave formation and weld growth, however, are separate from one another, according to some literary research. Due to similar metals, as the difference between ultimate strength and yield strength widens, so does the period of wave less welding. For dissimilar metals, the region of existence for the wavelength border of weld also develops as the strength property difference does[20]. The sample's average ultimate tensile strength in the welded condition was 110 mpa, and heat treatments were found to lower this value to 90 mpa.[21].

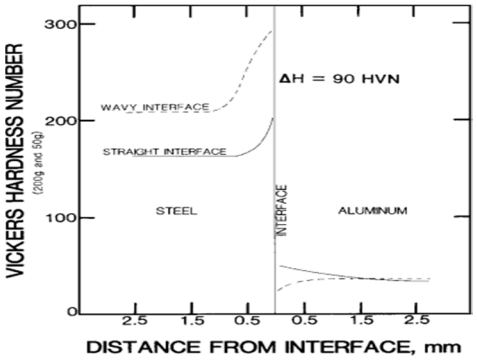

Fig. 19 Microhardness profiles for the as-welded straight and wavy AI-steel interfaces

There exist pressures in the collision zone above which metals act as viscous and in viscous liquids. Wave periodicity is caused by gradient in pressure zones. The joints become wary as a result of the frequent changes in angles and speed. The material from the plastic zone periodically leaks out as a result of the angle change[22].

Waves do not occur at the weld boundary when fusing steel and aluminum because the gap's reverse flow causes the tougher material's surface layers to deform[20]. In every test that resulted in breaking, it was observed that the joints with the wave less contact were made of aluminum[21]. The asymmetrical shape of the waves created at the contact is caused by the different densities of the two materials. With explosive welding, the wavelength and amplitude increase[23].

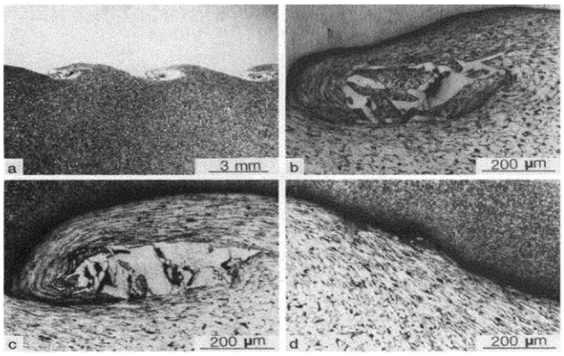

Fig.20- Wavy AI-steel explosively welded interface; the interface and the Fe-AI intermetallic are encapsulated at the vortex (a), (b), and (c) and on the aluminum plate (d) of the vortex.

Explosive-Welding Waves from the Self- Oscillation Standpoint. As the general theory of self- oscillations any self-oscillatory system must contain an oscillator with a certain frequency co and damping constant r 0. Moreover, there must be an energy pumping mechanism, which in actual systems is usually related to the presence of a nonlinear "negative" frictional resistance[24]. It is noted that the tensile strength of copper and stainless steel were obtained as 360 and 870 MPa, respectively[25].

Fig.22-Figure depicts mild steel plates used in shipbuilding (Figure 1a), traditional fusion welding in shipbuilding (Figure 1b), the FSW process of mild steel plates (Figure 1c), and a top view of an FSWed butt joint (Figure 1d) (Figure 1d)

G. Applications Of Friction Stir Welding

TWI first patented the FSW technology in the majority of industrialized countries and licensed it to over 183 clients. Friction stir welding and its variants, friction stir spot welding and friction stir processing, are used in the shipbuilding and offshore sectors, aerospace, automotive, railway rolling stock, general fabrication, robotics, and computers[26]. The Welding Institute (Cambridge) first enhanced friction stir welding (FSW), which allows metals to be joined without the need of filler or fusion material, in 1991[27].

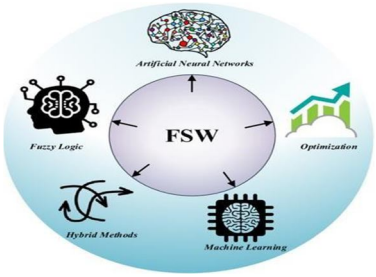

Fig. 21 FSW technology

H. Shipbuilding and offshore

Gas metal arc welding (GMAW) and shielded metal arc welding (SMAW) are the two welding techniques that are most often used in the shipbuilding industry. Friction stir welding (FSW) appears to be a superior option to conventional welding processes given its advantages. Steel materials have a high melting point, leading to the development of FSW tool designs and materials. The 1.6 mm butt-joint properties of ultra-low carbon (IF) steel and four different plain carbon sheets of steel (S12C, S20C, S35C, and S50C) were examined by Cui et al. using a tungsten carbide (WC) tool at FSW welding speeds ranging from 25 to 400 mm/min at a constant rotational speed of 400 rpm[28].

The technique proved very effective when used to aluminum alloys, which spurred curiosity in determining if it might also be used on other materials, such steel. Ghosh et al. published results for ordinary carbon steel (0.44% carbon content) when rotating and welding rates were changed. By utilizing single-sided one-pass butt welding, Matsushita et al. employed FSW on 12-mm thick structural steel grade plates with a tensile strength of 400 N mm2. For this experiment, the shipbuilding steel grade GL E36 was provided with uniform heat treatment conditions. 1200 mmL, 200 mmW, and 6 mmT plates were worked on in the rolling direction. using a butt joint design.

Table 1. The chemical make-up of the supplier[29]

Grade											
GL E36	C	Mn	Si	P	Cu	Ni	Cr	Mo	Al	N	Nb
0.170		1.400	0.390	0.013	0.030	0.020	0.060	0.006	0.027	0.007	0.025

Figures (a) through (d) in Figure 23 depict the oxidation and swelling behavior of WC material schematically. The oxidation behavior of the tungsten carbide tool may be explained using the equations below. 3 WC 5 2O2WO3 CO2 W C 2 O 2 W O 2O2WO3 CO4 WC In WC alloys, the oxidation processes are depicted in 4 Figures (a-d). When tungsten combines with oxygen near to the surface, it forms a porous tungsten oxide phase (WO3) and CO2 gas. The formation of a porous oxide layer speeds up the oxidation of the next layer. The outcome is that CO2 is contained inside the WC grains. Due to high pressures of CO2 gas and porous tungsten oxide (WO3), the ductile cobalt binder separates[30].

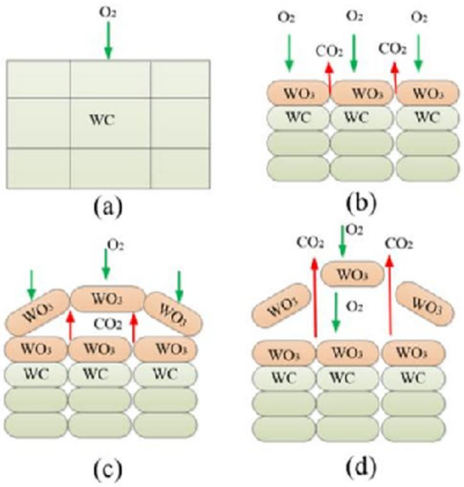

Figure 23a–d explains the oxidation phenomenon in WC alloys.

Because of its intrinsic features such as superior weldability, high strength-to-weight ratio, resistance to stress corrosion cracking, and outstanding mechanical properties across a wide temperature range. Generally, AA2219 propellant tanks are manufactured using tungsten inert gas welding (TIG) with ER 2319 filler wire and utilized as-welded[31].

I. Aerospace

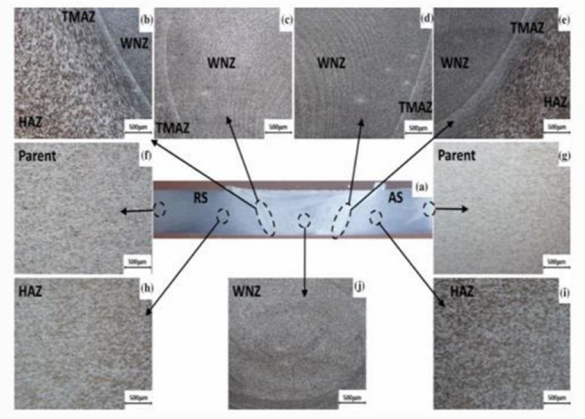

Fig 24 represents Schematic diagram of friction stir welding area

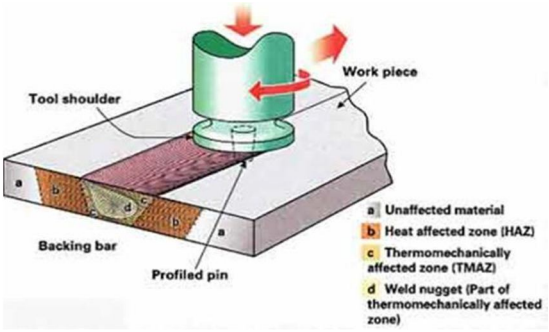

Fig. 25 Microstructures of the AA2219- T87 parent and FSW joint

Fig 25(a) FSW joint cross section, Fig 25(b), Fig 25(e) TMAZ-WNZ interface, Fig 25(c) and (d) WNZ displaying onion rings, and Fig 25(j) WNZ center showing fine recrystallized grains, Fig25(f) and (g) parent material, and Fig25(h) and I HAZ. In the diagram, AS represents the advancing side and RS represents the retreating side. The high-speed rotating tool softens the material in the welding zone plastically. As indicated in the picture, the highly flexible material behind the tool creates a tight weld connection under the forging force of the shoulder, with a portion of the material extruded above the workpiece during the first plunging stage. The tool enters the dwelling phase after a given amount of plunge, and a little amount of flash is readily created during welding owing to the extrusion of the shoulder[33].

J. Automotive

Steel and aluminum alloys have been joined using conventional welding techniques such arc welding, laser welding, and resistance spot welding, however with considerable limitations and drawbacks[34]. A solid-state joining technique called friction stir welding (FSW) has the ability to eliminate or significantly reduce the issues that are related to fusion welding procedures. Industrial hot-dip galvanized low carbon steel sheets (grade DC05) and sheets made of the aluminum alloy AA6016 were used in this investigation. For DC05 and AA6016, the sheets had a thickness of 0.8 and 1.0 mm, respectively. The chemical composition of these metals is shown in Table 2, while their mechanical properties are shown in Table 3[35].

Table 2. The chemical composition of the metals

	C	Mn	Si	P	S	Mg	Al	Fe
DC05	0.06	0.35	-	0.025	0.025	-	-	Bal.
AA6016	-	0.20	1.20	-	-	0.40	Bal.	-

Table 3. Mechanical properties of the metal

	Yield stress (YS) /MPa	Ultimate tensile strength (UTS) /MPa	Elongation at fracture, e_f /%	Hardness Vickers /HV1
DC05	155	300	43	105
AA6016	135	240	30	95

Achieving sound welding between them can contribute to a reduction in overall automobile weight, fuel consumption, and, as a result, CO2 emissions. The 950 RPM specimen had a groove- like flaw and shattered during cutting, thus it was not inspected further. The rectangular bilayer structure is 80 mm long and 27 mm broad, with an aspect ratio of around 3:1. Using CLT as a specific example of generalized plane strain, the following simplification may be made[36].

$$\begin{bmatrix} A_{11} & A_{12} & B_{22} \\ A_{12} & A_{22} & B_{12} \\ B_{11} & B_{12} & D_{11} \end{bmatrix} \begin{pmatrix} \varepsilon_x^0 \\ \varepsilon_y^0 \\ \kappa_x \end{pmatrix} = \begin{pmatrix} N_x^m \\ N_y^m \\ M_x^m \end{pmatrix}$$

$$M_y = B_{12}\varepsilon_x^0 + B_{22}\varepsilon_y^0 + D_{12}\kappa_x - M_y^m$$

The CLT-based analysis simply approximates it as a single value in this case. When compared to the elastic limit of Al-Mg-Si alloys at T4 conditions, which is 2.1 103, this figure for AFSD cladding on thin substrates is quite small. This discrepancy provides support to the idea that the solid-state nature of AFSD might result in lower thermal stresses[37],

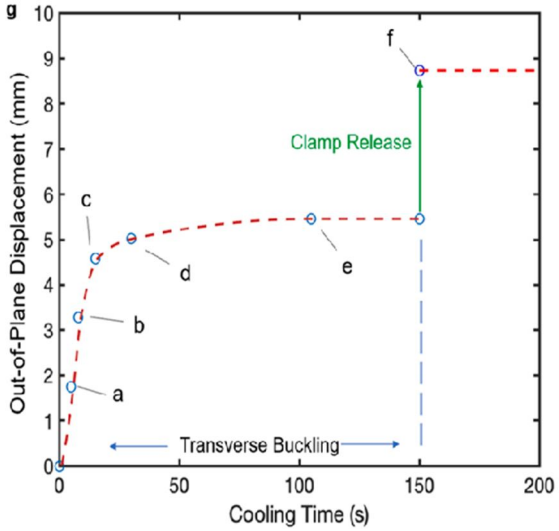

Fig 28 is, Plot of the out-of-plane displacement of the substrate centerline as a function of the cooling time. W.D. Hartley et al.

K. Railways

FSW is a solid-state welding technology that was designed to combine difficult-to-weld materials. Without the need of a filler, a solid-state welding technique uses plastic deformation to produce metallurgical bonds. Materia, Figure is a schematic depiction of a secondary vortex as illustrated by Chowdhury et al (a). Arbogast proposed that the FSW technique creates five distinct metalworking zones: I warmup zone (heated material upstream of the pin), (ii) commencing deformation zone (stress above the critical flow stress of the Fig. FSW process flowchart. Elsevier Inc. Eslami et al. (a) A secondary vortex forms around the pin during FSW. Elsevier's copyright (a) FSW metalworking zones[38].

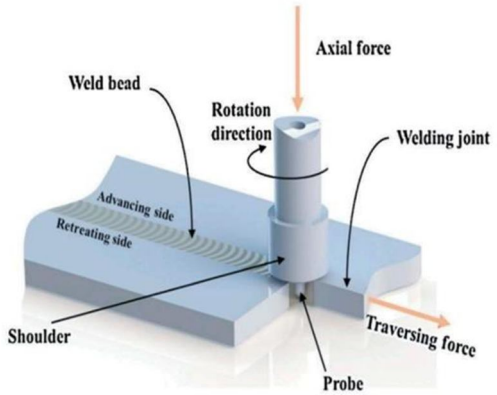

Fig 29 Represents Schematic of FSW Process

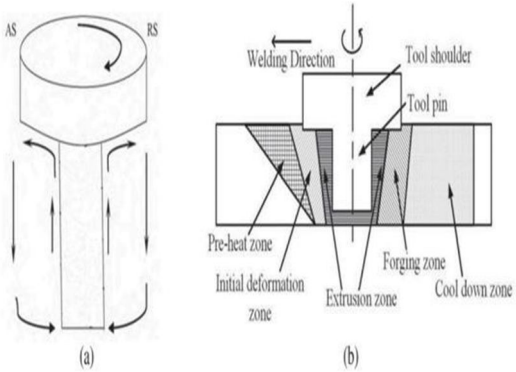

Fig 30 represents Material flow and different zones in FSW: (a) secondary vortex around pin during FSW b) metalworking zones in FSW

Although aluminum alloys have considerable corrosion resistance, even minor corrosion losses can contribute to a significant decline in the mechanical characteristics of the structure. Welding of dissimilar junctions was done at 100 mm/min constant tool traverse speed and 2o constant tool tilt angle. The rotational rates of the tools employed were 800, 1000, and 1200 RPM[39].

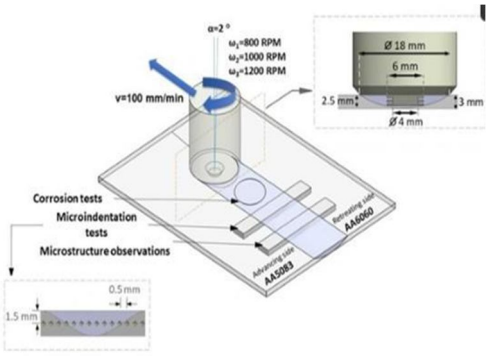

Fig. 31. FSW machine.

L. Fabrication

The bulk (92 weight percent) of the matrix materials employed in the creation of hybrid MMCs are AA6061, ZrO2 primary reinforcement materials, and C secondary reinforcement materials. Stir casting liquid metallurgy processes are used to create the hybrid MMCs. Table 1 lists the specs for the stir casting machine[40 -45].

ISSN: 2321-9653; IC Value: 45.98; SJ Impact Factor: 7.538
Volume 12 Issue VI June 2024- Available at www.ijraset.com

M. Stir Casting Process Parameter

Melting temperature	**10,000C**
Max stir speed	**500 rpm**
Linear movement of stir	**2/3rd of melt height**
Preheating temperature and time	**6000 C and 2h**

ZrO2 primary reinforcement materials make up 6% of the AA6061 used in the fabrication of hybrid MMCs, while C secondary reinforcement materials make up the remaining 2%. Metal matrix composites (MMCs) can be produced using a variety of methods, but the Stir Casting Process offers the best chances of achieving commercial goals.

N. Advantages Of Friction Stir Welding [46-55]

One advantage of friction stir welding (FSW) is that it uses less energy than arc welding techniques[6].

1) Metallurgical benefits

- Solid-phase process.
- Low distortion.
- No loss of alloying elements.
- Fine recrystallized microstructure.
- Absence solidification of cracking.
- Replaces multiple parts fasteners joined

2) Environmental Benefits

- Minimal surface cleaning required.
- Eliminates grinding wastes.
- Consumable material saving.
- No harmful emissions.

3) Energy Benefits

- Improved material use (e.g. joining different thickness) allows reduction in weight.
- Only 2.5% of the energy needed for a laser weld
- Decreased fuel consumption in lightweight aircraft, automotive, and Ship applications[7].

The use of friction stir welding in the manufacture of rocket fuel tanks significantly reduced welding costs63 and raised the calibre of welded joints[8].

4) *In Design and Manufacturing*

- Weight reductions - by doing away with sheet-overlap arrangements and rivets and other fasteners.
- Environmental requirements- less waste and less energy use[9].
- Due to the length of the weld, the needed travel speeds to make this process cost- competitive, and the accompanying process forces, this FSW application requires a customized linear machine. These machines have a high capital expenditure[10].

IX. CONCLUSION

Friction stir welding (FSW) represents a revolutionary advancement in joining dissimilar metals, offering a myriad of benefits over conventional welding techniques. Unlike traditional fusion methods, FSW operates at lower temperatures, minimizing thermal distortion and preserving the integrity of the base materials' microstructure. This results in joints with superior mechanical properties, including enhanced strength and toughness, as defects like porosity and cracks are significantly reduced. Moreover, FSW's versatility enables it to accommodate a wide range of dissimilar metal combinations, from aluminum to steel to titanium, expanding its applicability across diverse industries such as automotive, aerospace, and marine. Its environmentally friendly operation, characterized by minimal emissions and energy consumption, contributes to a cleaner and safer working environment. Although initial setup costs may be higher, FSW offers long-term cost savings through improved efficiency and reduced rework. Its ability to weld complex shapes and thin-walled structures further underscores its suitability for various applications, making FSW a preferred choice for joining dissimilar metals in modern manufacturing processes.

REFERENCES

[1] Ma, Z. Y. (2008). Friction stir processing technology: A review. In Metallurgical and Materials Transactions, A: Physical Metallurgy and Materials Science: Vol. 39 A (Issue 3, pp. 642–658). https://doi.org/10.1007/s11661-007-9459- 0
[2] Simar, A., & Avettand-Fènoël, M. N. (2017). State of the art about dissimilar metal friction stir welding. In Science and Technology of Welding and Joining (Vol. 22, Issue 5, pp. 389–403). Taylor and Francis Ltd.https://doi.org/10.1080/13621718.2016.12 51712
[3] Storjohann, D., Barabash, O. M., Babu, S. S., David, S. A., Sklad, P. S., & Bloom, E. E. (n.d.). Fusion and Friction Stir Welding of Aluminum-Metal-Matrix Composites.
[4] Mahoney, M. W., Rhodes, C. G., Flintoff, J. G., Spurling, R. A., & Bingel, W. H. (1998). Properties of Friction-Stir-Welded 7075 T651 Aluminum.
[5] Hwang, Y. M., Fan, P. L., & Lin, C. H. (2010). Experimental study on Friction Stir Welding of copper metals. Journal of Materials Processing Technology, 210(12),1667–1672. https://doi.org/10.1016/j.jmatprotec.2010. 05.019
[6] Nandan, R., DebRoy, T., & Bhadeshia, H. K. D. H. (2008). Recent advances in friction-stir welding - Process, weldment structure and properties. In Progress in Materials Science (Vol. 53, Issue 6, pp. 980–1023). https://doi.org/10.1016/j.pmatsci.2008.05. 001
[7] Akinlabi, E. T. (2012). Effect of shoulder size on weld properties of dissimilar metal friction stir welds. Journal of Materials Engineering and Performance, 21(7), 1514–1519. https://doi.org/10.1007/s11665-011-0046- 6
[8] Shtrikman, M. M. (2008). Current state and development of friction stir welding Part 3. Industrial application of friction stir welding. Welding International, 22(11), 806–815. https://doi.org/10.1080/095071108025936 20
[9] Shtrikman, M. M. (2008). Current state and development of friction stir welding Part 3. Industrial application of friction stir welding. Welding International, 22(11), 806–815. https://doi.org/10.1080/095071108025936 20
[10] Sinka, V. (2014). The present and future prospects of friction stir welding in aeronautics. Acta Metallurgica Slovaca, 20(3), 287–294. https://doi.org/10.12776/ams.v20i3.312
[11] Noruk, J. (n.d.). FRICTION STIR WELDING INTHE AUTOMOTIVE INDUSTRY. https://www.researchgate.net/publication/2 68325940
[12] Lucaci, M., Leonat, L., & Alecu, G. (2007). International conference Innovative technologies for joining advanced materials MATERIALS BONDING BY DIFFUSION WELDING TECHNOLOGY. https://www.researchgate.net/publication/2 80776509
[13] Kolukisa, S. (2007). The effect of the welding temperature on the weldability in diffusion welding of martensitic (AISI 420) stainless steel with ductile (spheroidal graphite-nodular) cast iron. Journal of Materials Processing Technology, 186(1– 3),33–36. https://doi.org/10.1016/j.jmatprotec.2006. 11.148
[14] Shi, H., Qiao, S., Qiu, R., Zhang, X., & Yu, H. (2012). Effect of welding time on the joining phenomena of diffusion welded joint between aluminum alloy and stainless steel. Materials and Manufacturing Processes, 27(12), 1366–1369. https://doi.org/10.1080/10426914.2012.66 3122
[15] Shtrikman, M. M. (2008). Current state and development of friction stir welding Part 3. Industrial application of friction stir welding. Welding International, 22(11), 806–815. https://doi.org/10.1080/095071108025936 20
[16] Sinka, V. (2014). The present and future prospects of friction stir welding in aeronautics. Acta Metallurgica Slovaca, 20(3), 287–294. https://doi.org/10.12776/ams.v20i3.312
[17] Sinka, V. (2014). The present and future prospects of friction stir welding in aeronautics. Acta Metallurgica Slovaca, 20(3), 287–294. https://doi.org/10.12776/ams.v20i3.312
[18] Noruk, J. (n.d.). FRICTION STIR WELDING IN THE AUTOMOTIVE INDUSTRY. https://www.researchgate.net/publication/2 68325940
[19] Lucaci, M., Leonat, L., & Alecu, G. (2007). International conference Innovative technologies for joining advanced materials MATERIALS BONDING BY DIFFUSION WELDING TECHNOLOGY. https://www.researchgate.net/publication/2 80776509
[20] Kolukisa, S. (2007). The effect of the welding temperature on the weldability in diffusion welding of martensitic (AISI 420) stainless steel with ductile (spheroidal graphite-nodular) cast iron. Journal of Materials Processing Technology, 186(1– 3),33–36. https://doi.org/10.1016/j.jmatprotec.2006. 11.148
[21] Shi, H., Qiao, S., Qiu, R., Zhang, X., & Yu, H. (2012). Effect of welding time on the joining phenomena of diffusion welded joint between aluminum alloy and stainless steel. Materials and Manufacturing Processes, 27(12), 1366–1369. https://doi.org/10.1080/10426914.2012.66 3122
[22] Wronka, B. (2010). Testing of explosive welding and welded joints. the microstructure of explosive welded joints and their mechanical properties. Journal of Materials Science, 45(13), 3465–3469. https://doi.org/10.1007/s10853-010-4374- y
[23] Wronka, B. (2010). Testing of explosive welding and welded joints. the microstructure of explosive welded joints and their

mechanical properties. Journal of Materials Science, 45(13), 3465–3469. https://doi.org/10.1007/s10853-010-4374- y
[24] Chinesta, Francisco., Chastel, Yvan., & Mansori, M. El. (2010). International conference on advances in materials and processing technologies : AMPT2010, 24- 27 October 2010, Paris, France. American Institute of Physics.
[25] Findik, F. (2011). Recent developments in explosive welding. In Materials and Design (Vol. 32, Issue 3, pp. 1081–1093). https://doi.org/10.1016/j.matdes.2010.10.0 17
[26] Eren, B., Guvenc, M. A., & Mistikoglu, S. (2021). Artificial Intelligence Applications for Friction Stir Welding: A Review. In Metals and Materials International (Vol. 27, Issue 2, pp. 193–219). Korean Institute of Metals and Materials. https://doi.org/10.1007/s12540-020- 00854-y
[27] Mahesh Reddy, D., Anitha Lakshmi, A., & Ul Haq, A. (2019). Experimental Taguchi approach and Gray-Taguchi optimization on mechanical properties of aluminum 8011 alloy sheet under uniaxial tensile loads. Materials Today: Proceedings, 19, 366–371. https://doi.org/10.1016/j.matpr.2019.07.61 4
[28] Findik, F. (2011). Recent developments in explosive welding. In Materials and Design (Vol. 32, Issue 3, pp. 1081–1093). https://doi.org/10.1016/j.matdes.2010.10.0 17
[29] Eren, B., Guvenc, M. A., & Mistikoglu, S. (2021). Artificial Intelligence Applications for Friction Stir Welding: A Review. In Metals and Materials International (Vol. 27, Issue 2, pp. 193–219). Korean Institute of Metals and Materials. https://doi.org/10.1007/s12540-020- 00854-y
[30] Tiwari, A., Pankaj, P., Biswas, P., Kore, S. D., & Rao, A. G. (2019). Tool performance evaluation of friction stir welded shipbuilding grade DH36 steel butt joints. International Journal of Advanced Manufacturing Technology, 103(5–8), 1989–2005. https://doi.org/10.1007/s00170-019- 03618-0
[31] Manikandan, P., Prabhu, T. A., Manwatkar, S. K., Rao, G. S., Murty, S. V. S. N., Sivakumar, D., Pant, B., & Mohan, M. (2021). Tensile and Fracture Properties of Aluminium Alloy AA2219-T87 Friction Stir Weld Joints for Aerospace Applications. Metallurgical and Materials Transactions A: Physical Metallurgy and Materials Science, 52(9), 3759–3776. https://doi.org/10.1007/s11661-021- 06337-y
[32] Elkoushy, M. A., Metwally, A. H., & Noureldin, Y. A. (2016). Implications of different nephrolithometry scoring systems on clinical practice of endourologists: An international web-based survey. Arab Journal of Urology, 14(3), 216–222. https://doi.org/10.1016/j.aju.2016.04.005
[33] Wu, T., Zhao, F., Luo, H., Wang, H., & Li, Y. (2019). Temperature monitoring and material flow characteristics of friction stir welded 2A14-t6 aerospace aluminum alloy. Material12(20).
https://doi.org/10.3390/ma12203387
[34] Safeen, M. W., Russo Spena, P., Buffa, G., Campanella, D., Masnata, A., & Fratini, L. (2020). Effect of position and force tool control in friction stir welding of dissimilar aluminum-steel lap joints for automotive applications. Advances in Manufacturing, 8(1), 59–71.
https://doi.org/10.1007/s40436-019- 00290-1
[35] Karakizis, P. N., Pantelis, D. I., Dragatogiannis, D. A., Bougiouri, V. D., & Charitidis, C. A. (2019). Study of friction stir butt welding between thin plates of AA5754 and mild steel for automotive applications. International Journal of Advanced Manufacturing Technology, 102(9–12), 3065–3076. https://doi.org/10.1007/s00170-019- 03388-9
[36] Hartley, W. D., Garcia, D., Yoder, J. K., Poczatek, E., Forsmark, J. H., Luckey, S. G., Dillard, D. A., & Yu, H. Z. (2021). Solid-state cladding on thin automotive sheet metals enabled by additive friction stir deposition. Journal of Materials Processing Technology, 291.
https://doi.org/10.1016/j.jmatprotec.2021. 117045
[37] Hartley, W. D., Garcia, D., Yoder, J. K., Poczatek, E., Forsmark, J. H., Luckey, S. G., Dillard, D. A., & Yu, H. Z. (2021). Solid-state cladding on thin automotive sheet metals enabled by additive friction stir deposition. Journal of materials processing technology, 291.
https://doi.org/10.1016/j.jmatprotec.2021.117045
[38] Bhardwaj, N., Narayanan, R. G., Dixit, U. S., & Hashmi, M. S. J. (2019). Recent developments in friction stir welding and resulting industrial practices. In Advances in Materials and Processing Technologies. (Vol. 5, Issue 3, pp. 461-496). Taylor and Francis Ltd
[39] G, R. H., Byregowda, H. v, & Kumar M, S. N. (n.d.). Optimization of ZnO Thin Films using Sol-Gel Dip Coating by Taguchi Method Section A-Research paper ISSN. In Eur. Chem. Bull. 2023 (Vol. 12, Issue 8).
[40] Siddesh Kumar, N. M., Dhruthi, Pramod, G. K., Samrat, P., & Sadashiva, M. (2022). A Critical Review on Heat Treatment of Aluminium Alloys. Materials Today: Proceedings, 58, 71–79. https://doi.org/10.1016/j.matpr.2021.12.586
[41] Shivaprakash, Y. M., Gurumurthy, B. M., Siddhartha, M. A., Kumar, N. M. S., & Dutta, A. (n.d.). STUDIES ON MILD STEEL PARTICULATES REINFORCED DURALUMIN COMPOSITE FABRICATED THROUGH POWDER METALLURGY ROUTE. In www.tjprc.org SCOPUS Indexed Journal editor@tjprc.org. www.tjprc.org
[42] Kumar, N. M. S., Shashank, T. N., Dheeraj, N. U., Dhruthi, Kordijazi, A., Rohatgi, P. K., & Sadashiva, M. (2023). Coatings on Reinforcements in Aluminum Metal Matrix Composites. International Journal of Metalcasting, 17(2), 1049–1064. https://doi.org/10.1007/s40962-022-00831-8
[43] Kumar M, S. N., & Bawge, G. (n.d.). Comparitive Study on Methods used to Improve the Corrosion Resistance Property of Aluminium Alloys-A Review. www.solidstatetechnology.us
[44] Siddesh Kumar, N. M., Chethan, S., Nikhil, T., & Dhruthi. (2022). A review on friction stir processing over other surface modification processing techniques of magnesium alloys. In Functional Composites and Structures (Vol. 4, Issue 1). IOP Publishing Ltd. https://doi.org/10.1088/2631-6331/ac49f3
[45] Siddesh Kumar, N. M. (2022). Effect on wear property of aluminium metal matrix composite reinforced with different solid lubricants: a review. In International Journal of System Assurance Engineering and Management. Springer. https://doi.org/10.1007/s13198-022-01654-w
[46] Murthy, L. N. H. R., Kurbet, R., Kumar, S. N. M., Jashwanth, K., & Bhargav, P. (2022). Parametric Based Influence of Silicon Carbide Particulates on Tensile and Hardness Characteristics of Graphitic Aluminium Copper Alloy. AIP Conference Proceedings,2648. https://doi.org/10.1063/5.0118021
[47] G, R. H., Byregowda, H. v, & Kumar M, S. N. (n.d.). Optimization of ZnO Thin Films using Sol-Gel Dip Coating by Taguchi Method Section A-Research paper ISSN. In Eur. Chem. Bull. 2023 (Vol. 12, Issue 8)
[48] Siddesh Kumar, N. M., Sadashiva, M., Monica, J., & Praveen Kumar, S. (2021). Investigation on Corrosion Behaviour of Hybrid Aluminium Metal Matrix Composite Welded by Friction Stir Welding. Materials Today: Proceedings, 52,2339–2344. https://doi.org/10.1016/j.matpr.2022.01.362
[49] Sadashiva, M., Siddeshkumar, N. 50. Sadashiva, M., Siddeshkumar, N. M.,Monica, J., Srinivasa, M. R., Santhosh, N., & Praveenkumar, S. (2022). Hardness and Impact Strength Characteristics of Al based Hybrid Composite FSW Joints. International Journal of Vehicle Structures and Systems, 14(1), 13–17. https://doi.org/10.4273/ijvss.14.1.04
[50] Kurbet, R., Doddaswamy, V., Amruth, C. M., Kerur, M. H., & Ghanaraja, S. (2022). Frequency response analysis of spur gear pair using FEA. Materials

Today: Proceedings, 52, 2327-2338.
[51] Kurbet, R., Basavaraj, Amruth, C. M., & Jayasimha, S. L. N. (2022). Effect of Ceramic Particles on AMMC Through Stir Casting Method—A Review (pp. 373–388). https://doi.org/10.1007/978-981-16-4321-7_3
[52] Kumar M, P. B., Aatifulla Baig, M. M., Dharawadmath, S. I., & M, V. C. (2023). Review on Current Applications and Future Directions in Carbon Nanotubes for Cancer Therapy using AI. 11. www.ijraset.com
[53] Kalal, P., K, A. M., Dharawadmath, S. I., & M, V. C. (2023). Modern Smart Street Light Monitoring Systems. 11. www.ijraset.com
[54] Kurbet, R., Doddaswamy, V., Amruth, C. M., Kerur, M. H., & Ghanaraja, S. (2022). Frequency response analysis of spur gear pair using FEA. Materials Today: Proceedings, 52, 2327-2338.
[55] Kurbet, R., Basavaraj, Amruth, C. M., & Jayasimha, S. L. N. (2022). Effect of ceramic particles on AMMC through stir casting method—a review. In Proceedings of Fourth International Conference on Inventive Material Science Applications: ICIMA 2021 (pp. 373-388). Springer Singapore.
[56] Kurbet, R., Karthikareddy, G., & Monica, J. (2021). A Review on Friction Stir Welding over other Welding Techniques of Aluminium Alloys. Solid state technology, 64(2), 3713-3729.
[57] Madhyastha, P. R., Kurbet, R., & SL, A. P. (2020). Vibrational and Noise Signal Analysis to Detect the Gear Teeth Damage in A Gear Box with Austempered Ductile Iron as Gear Material. Research and Development in Machine Design, 3(2).
[58] NR, K. K., Dharmaraj, H. S., KI, S. A., Kurbet, R., & SL, A. P. (2020). Vibration and Noise Signal Analysis of Al-SiC MMC Gears. Research and Development in Machine Design, 3(2).
[59] Madhyastha, P. R., Kurbet, R., & Prasad, S. A. (2020). Detection and Identification of Gear Teeth Damage through Sound and Vibration Signal Analysis of Austempered Ductile Iron Gear. International Research Journal of Engineering and Technology, 7(8), 1839-1844.
[60] KI, S. A., Kurbet, R., & SL, A. P. (2020). Fault Diagnosis of Gearbox Having Delrin Gear by Vibration and Noise Signal Analysis. Research and Development in Machine Design, 3(2).
[61] Patil, P. B., Humbi, N., Kurbet, R., Goggal, P. V., & Jadhav, C. C. (2024, March). Work in Progress: Impact of Design Thinking on Creativity Amongst First-Year Undergraduate Engineering Students. In 2024 IEEE World Engineering Education Conference (EDUNINE) (pp. 1-4). IEEE.
[62] Channangi, S. M., Kurbet, R., Humbi, N., Patil, P. B., Jadhav, C. C., Goggal, P. V., & Udapudi, P. (2024, March). Work in Progress: Enhancing Engineering Students' Learning in PjBL Courses through Electronic Testing Kits. In 2024 IEEE World Engineering Education Conference (EDUNINE) (pp. 1-4). IEEE.
[63] Humbi, N., Patil, P. B., Kurbet, R., Jadhav, C., & Goggal, P. (2024, March). First-Year Undergraduate Engineering Student's Investigation on the Troubleshooting Process in a Project Based Learning Course. In 2024 IEEE World Engineering Education Conference (EDUNINE) (pp. 1-5). IEEE.
[64] Goggal, P., Patil, P. B., Kurbet, R., Humbi, N., & Jadhav, C. (2024, March). A Review on the Importance of Article Writing for Engineering Students. In 2024 IEEE World Engineering Education Conference (EDUNINE) (pp. 1-5). IEEE.
[65] Salunkea, R., Goudarb, N., Kurbetc, R., Goggald, P. V., & Ghokhalee, S. (2024). Awareness of Divyanga Seva Kendra among physically impaired in Hubli-Dharwad region. Journal of Engineering Education Transformations, 37(Special Issue 2).
[66] Kurbet, R., HR, A., Holagi, S., & KS, V. (2023). Applications of Robotic in Industry-A Review. Journal of Mines, Metals & Fuels, 71(6).
[67] Lakshmi Narasimha Murthy, H. R., Kurbet, R., Siddesh Kumar, N. M., Jashwanth, K., & Bhargav, P. (2022, November). Parametric based influence of silicon carbide particulates on tensile and hardness characteristics of graphitic aluminium copper alloy. In AIP Conference Proceedings (Vol. 2648, No. 1). AIP Publishing

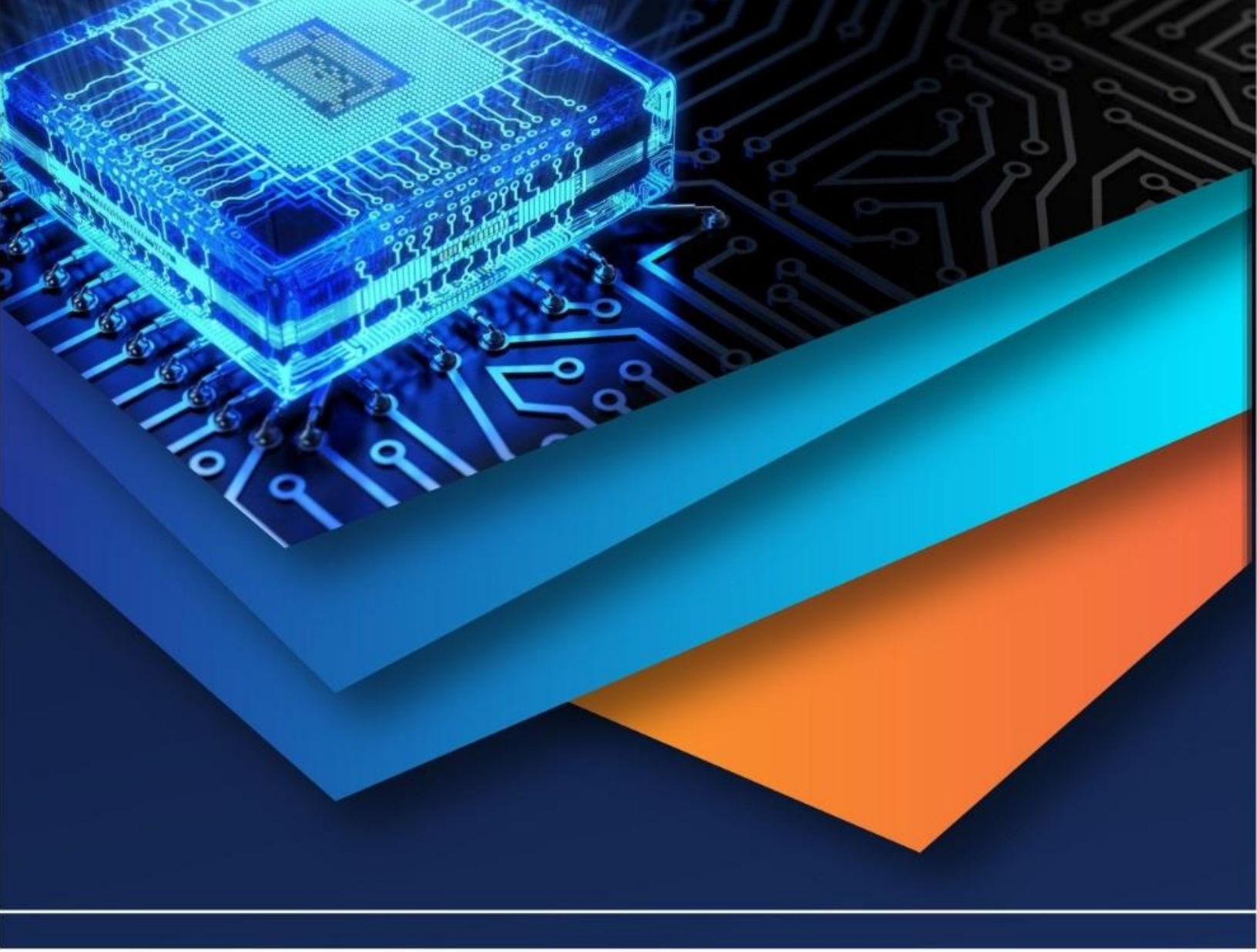

10.22214/IJRASET

45.98

IMPACT FACTOR: 7.129

IMPACT FACTOR: 7.429

INTERNATIONAL JOURNAL FOR RESEARCH

IN APPLIED SCIENCE & ENGINEERING TECHNOLOGY